Determination of Early Age Mortar and Concrete Strength by Ultrasonic Wave Reflections

Thomas Voigt[1], Yilmaz Akkaya[2], Surendra P. Shah[3]

Keywords: nondestructive tests, ultrasonic tests, compressive strength, concrete, mortars, hydration, wave reflection, transverse waves

ABSTRACT

The in-situ testing of early age concrete strength is crucial for determining the time of form removal from concrete elements, opening highways to traffic or applying of prestress to steel reinforcement. A nondestructive ultrasonic technique, which measures the reflection loss of ultrasonic transverse waves at a concrete-steel interface, is presented in this paper. The focus is to compare wave reflection measurements on mortar and concrete to strength. It is shown that the reflection loss is linearly related to the strength gain of mortar and concrete at early ages. The experiments have revealed a relationship between the homogeneity of the tested materials and the consistency of the reflection measurements. The repetition of simultaneous measurements of wave reflections and compressive strength on mortar results in similar strength-reflection loss relationships. Multiple measurements on the same concrete gave multiple strength-reflection loss relationships. The accuracy of the strength predictions made with the proposed method is discussed and compared to other nondestructive test methods.

[1] Dipl.-Ing., Research Associate, Center for Advanced Cement-Based Materials, Northwestern University, 2145 Sheridan Road, Evanston, Illinois 60208. Email: th-voigt@northwestern.edu, Corresponding Author

[2] Ph.D., Research Associate, Center for Advanced Cement-Based Materials, Northwestern University, 2145 Sheridan Road, Evanston, Illinois 60208. Currently at Istanbul Technical University, Civil Engineering Faculty, Maslak, 80626, Istanbul, Turkey. Email: yakkay@northwestern.edu

[3] Prof. for Civil Engineering, Director of Center for Advanced Cement-Based Materials, Northwestern University, 2145 Sheridan Road, Evanston, Illinois 60208. Email: s-shah@northwestern.edu.

INTRODUCTION

The technological progress of the last decade has brought a tremendous change to many fields of the civil engineering sciences. A representative indicator is the development of numerous sophisticated techniques for nondestructive testing of cementitious materials. The great variety of methods is based on acoustical, electrical, magnetic, mechanical, optical, radiographic, and thermal properties of the tested materials. This paper reports on a wave reflection method based on ultrasonic wave propagation. In the following, a short overview is given about the development of the method and various applications of this technique that can be found in the literature.

Papadakis (1968) described experiments with a buffer rod bonded to a sample material. A transducer at the free end of the buffer rod was used to generate ultrasonic waves and to monitor the reflections from the buffer-sample interface and from the far end of the sample. From the amplitude ratios of certain echoes the reflection coefficient at the interface and the ultrasonic attenuation in the sample were calculated.

The first application of the method to cementitious materials was reported by Stepišnik et al. (1981). The reflections of transverse waves (T-waves) at the interface between a quartz bar and cement paste were monitored and used to calculate the reflection coefficient at the interface as well as the shear modulus and dynamic viscosity of the cement paste. The measured quantities were found to be sensitive indicators of the hydration process at early ages. Based on these experiments Valič and Stepišnik (1998, 1999) have investigated the hydration of gypsum, various types of cement pastes and epoxy. In another study Valič (2000) investigated the hydration of cement paste as it is affected by different admixtures. The measurement of the reflection coefficient could reflect the various hydration kinetics.

Öztürk et al. (1999) adapted the wave reflection technique to concrete. The reflection coefficient was calculated from T-wave reflections at the interface between the concrete and a steel plate. The values of the reflection coefficient of concretes containing different admixtures were correlated to pin penetration tests and concrete temperature measurements. A distinct point in the development of the reflection coefficient was found to be related to the initial setting time and the end of the induction period in the hydration process. In continuation of this work Rapoport et al. (2000) advanced this theory further and additionally compared the development of the shear moduli determined by wave reflection measurements and the vibrational resonance frequency method. The wave reflection method as described in these papers has a high potential for further field applications.

A combined study of the hydration process of cement paste is reported by Chotard et al. (2001). The experimental setup is similar to that introduced by Papadakis (1968). The reflection coefficient and the longitudinal wave (L-wave) velocity was compared to results from shrinkage measurements, X-ray diffraction, differential thermal analysis and thermogravimetric measurements. The ultrasonic parameters proved to be sensitive to the formation and structuring of hydration products.

In a recent study by Akkaya et al. (2002) the wave reflection method was used to monitor the strength development of concrete. The compressive strength was found to be linearly related to the wave reflection measurements performed under isothermal and outdoor conditions and a

procedure for the strength prediction was developed. The experiments have shown that the method can reliably assess the early-age strength gain of concrete.

PHYSICAL INTERPRETATION OF THE REFLECTION COEFFICIENT

The wave reflection method monitors the development of the reflection coefficient at the interface between two materials over time. When a longitudinal or transverse wave is reflected at a boundary between Material 1 and Material 2 the reflection coefficient r can be calculated as

$$r = \frac{\rho_2 v_2 - \rho_1 v_1}{\rho_2 v_2 + \rho_1 v_1} \tag{1}$$

where ρ_1 and ρ_2 are the density of the Materials 1 and 2 and v_1 and v_2 the wave velocity in the Materials 1 and 2 respectively. Knowing the density ρ and the T-wave velocity v_T of a material the dynamic shear modulus can be calculated as follows:

$$G = \rho \cdot v_T^2 . \tag{2}$$

The interconnection of r and G expressed by Equations 1 and 2 shows that the reflection coefficient measured with transverse waves can theoretically be related to dynamic shear modulus G. Consequently, the reflection coefficient determined with transverse waves is governed by the development of the dynamic shear modulus. The development of shear modulus as a mechanical property of the material is related to how the microstructure of hydrating cement evolves as a result of curing. The compressive strength of cementitious materials also depends on the progress of the cement hydration. Accordingly, with reflection coefficient and compressive strength, two parameters with a direct physical relationship to the evolving properties of the test material are compared.

EXPERIMENTAL PROCEDURE AND APPARATUS

The experiments described in this paper are based on wave reflection measurements at an interface between a buffer material and a cementitious test material (e.g. concrete). For all experiments the wall or bottom plate of a steel mold (wall thickness = 12 mm) was used as the buffer material. The dimensions of the mold are 10x8x41 cm. A transducer with a center frequency of 2.25 MHz transmits a T-wave pulse into the steel. When the wave encounters the steel-concrete interface, part of the wave energy is transmitted into the concrete and part is reflected back to the transducer. Some of this wave energy is then again reflected from the transducer-steel interface into the steel and is again partially reflected when it hits the steel-concrete boundary. The described process is shown in Fig. 1, where S_T is the Transducer signal transmitted into the steel, R_1 and R_2 are the first and second reflection captured by the transducer and T_1 and T_2 are the first and second transmission into the concrete.

The measurements start directly after placing the fresh concrete. When the concrete is liquid, the entire wave energy, which is approaching the interface, is reflected, since T-waves cannot propagate in liquids. Thus, the reflection coefficient is unity. With proceeding hydration

the cement grains percolate and build up a skeleton allowing the T-waves to propagate. With increasing hydration time the ability of the concrete to transmit T-waves gains higher levels. More and more wave energy is transmitted into the concrete and the reflection coefficient decreases rapidly. After a certain time this process slows down and the reflection coefficient approaches a final value. At this time changes in the microstructure of the concrete due to hydration are too small to alter the T-wave propagation properties significantly.

The reflections R_1 and R_2 are acquired in time domain (Fig. 2(a)) and then transformed into frequency domain using a fast Fourier transform (FFT) algorithm (Fig. 2(b)). The separation of the reflections in time domain for the given steel plate thickness is about 7 μs. The reflection factor is calculated from the first and second reflections represented in frequency domain. The following procedure is applied to isolate the reflection coefficient. The first reflection can be written as

$$F_1(f) = S_T \cdot d_1 \cdot r \cdot d_2 \tag{3}$$

where $F_1(f)$ is the FFT of the first reflection in terms of the frequency f; S_T the transducer function including transducer specific variables and variables due to coupling; r the reflection coefficient at the steel concrete interface and d_1 and d_2 express the material and geometric signal losses along the propagation path through the steel to and from the interface. The second reflection is given by

$$F_2(f) = S_T \cdot d_1 \cdot r \cdot d_2 \cdot \bar{r} \cdot d_3 \cdot r \cdot d_4 \tag{4}$$

where $F_2(f)$ is the FFT of the second reflection in terms of the frequency f; $\bar{r}$ the reflection coefficient at the transducer-steel interface; and d_3 and d_4 are again the material and geometric signal losses along the corresponding wave paths. Calculating the ratio of $F_2(f)/F_1(f)$ is not sufficient to determine the reflection coefficient, since d_3, $\bar{r}$ and d_4 remain in the expression. To remove these factors experiments on an empty mold must be performed. For this free boundary case, where the reflection coefficient at the steel-air interface is unity, the ratio of the second to the first signal results in

$$\frac{F_{2,free}(f)}{F_{1,free}(f)} = \frac{S_T \cdot d_1 \cdot 1 \cdot d_2 \cdot \bar{r} \cdot d_3 \cdot 1 \cdot d_4}{S_T \cdot d_1 \cdot 1 \cdot d_2} = d_3 \cdot \bar{r} \cdot d_4 \tag{5}$$

where $F_{1,free}(f)$ and $F_{2,free}(f)$ are the FFT of the first and second reflection for the free boundary case, respectively. By dividing the ratio derived from Equation 3 and 4 by the ratio for the free boundary case (Equation 5) the reflection coefficient can be isolated. The presented algorithm is also explained in detail by Öztürk et al. (1999).

Basically, the reflection coefficient as calculated above represents an amplitude ratio and describes the relative loss in amplitude between the first and second reflection at a given time t. In ultrasonics amplitude ratios are usually measured in decibel (Krautkrämer and Krautkrämer, 1990). The reflection coefficient r(t) expressed in decibel becomes the reflection loss $R_L(t)$. The conversion of r into R_L can be done with

$$R_L(t) = -20 \cdot \log(r(t)) \tag{6}$$

with $R_L(t)$ as the reflection loss at time t and r(t) as the reflection coefficient at time t. For all further elaborations in this paper, the reflection coefficient is expressed in terms of the reflection loss.

EXPERIMENTAL PROGRAM

In order to analyze and compare wave reflection measurements on mortar and concrete, experiments with three different batches of one mortar and one concrete mixture were performed under constant temperature conditions. Simultaneously to the wave reflection measurements, the compressive strength was determined by compression tests. The tests were performed at least every 3 hours between 12 and 24 hours after casting and after that every 12 hours until the end of 3 days. The strength was calculated from the average of three compression tests on standard cylinders (76 mm diameter and 152 mm height) at one time. Portland cement type I, gravel with a maximum aggregate size of 16 mm, river sand and fly ash class F was used as ingredients for the mortar and concrete mixtures. The composition of the mixtures is given in Table 1.

RESULTS

The reflection loss curves measured on the three batches of mortar (M-1,2,3) and concrete (C-1,2,3) of identical composition are shown in Figs. 3 and 4. It is apparent that the measurements on the mortar samples show a very good repeatability. All three reflection loss graphs for mortar are consistent in shape and converge to a unique, material-specific asymptote. In contrast to mortar, the reflection loss curves for the three tested concrete samples bear resemblance only in respect of their shape. Thus the time of occurrence of distinctive points in the reflection loss graph is reproduced. But the repeatability is lacking in regard to the final value of the reflection loss. All three samples approach three different final values.

This result suggests that the homogeneity of the material and the consistency of the final reflection loss value are connected. The measurements on the relatively homogeneous mortar give a unique reflection loss development, where the experiments with the inhomogeneous concrete are not consistent in the final value. It is assumed that local differences in w/c-ratio, cement and paste content and aggregate dispersion are responsible for this phenomenon.

The strength development of the mortar and concrete mixture is presented in Fig. 5. The sensitivity of the reflection loss to the strength development can be clarified by comparing the patterns of the strength and reflection loss curves. The higher compressive strength of the mortar in the first 24 hours is reflected in the measured reflection loss. The curves for mortar shown in Fig. 3 start to increase earlier than the curves for concrete in Fig. 4.

STRENGTH PREDICTION PROCEDURE

To predict the compressive strength from the measured reflection loss, a direct relationship between those quantities needs to be established. The correlation between the compressive strength and reflection loss of experiment M-2 at early age is given in Fig. 6(c). The relationship exhibits a clear linear trend, which is an essential finding for the further

development of the strength prediction procedure. For the purpose of simplification of the prediction algorithm, this relationship shall be transformed into a interdependence of strength and the change of reflection loss (S-ΔR_L relationship), which passes the origin. The change of reflection loss is calculated as the difference between the reflection loss RL(t) at a certain time and a critical reflection loss value $R_{L,crit}$ at that time when strength theoretically starts to increase.

There are two possibilities to determine $R_{L,crit}$. The first alternative is to define it as the intersection of the strength–reflection loss relationship with the reflection loss axis (Fig. 6(c)). However, this requires the knowledge of a considerable part of the experimentally determined compressive strength development. The critical reflection loss value established this way shall be denoted as $R_L(t_s)$.

The second option to determine $R_{L,crit}$ is by analyzing only the reflection loss curve presented in Fig. 6(b). The first derivative of the reflection loss curve exhibits a maximum (Fig. 6(a)), which coincides with the point of inflection in the reflection loss graph. Later in this chapter, it is shown that the time of occurrence of this inflection point is related to the time t_s which marks the occurrence of $R_L(t_s)$ discussed in the previous paragraph. The critical reflection loss value determined by using only the inflection point of the reflection loss curve shall be denoted as $R_L(t_i)$.

To show the potential of the proposed method for the strength prediction the first alternative will be used to determine the critical reflection loss value ($R_{L,crit}= R_L(t_s)$). This will give the most accurate prediction results, but is indeed impossible without a number of accompanying strength tests.

When the S-ΔR_L relationship is found, the compressive strength for any time $t > t_s$ can be predicted from the reflection loss measurements. The equation of the S-ΔR_L relationship is

$$S(t) = m \cdot \Delta A(t) \tag{7}$$

$$\text{with:} \quad \Delta A(t) = \left[A(t) - A(t_s)\right] \tag{8}$$

where S(t) is the predicted strength at time t, m the slope of the S-ΔR_L relationship, and $R_L(t)$ and $R_L(t_s)$ the reflection loss at time t and t_s respectively. Further details of determination of the S-ΔR_L relationship can also be found in Akkaya et al. (2002).

A separate S-ΔR_L relationship was determined for each of the mortar and concrete batches by linear least square regression of compressive strength on the change of reflection loss. In Table 2 the time values t_i, t_s and their ratios are given. The ratio of t_s to t_i is not a fixed quantity, but is clearly limited to a certain range (0.66 – 0.75 in this study). This illustrates a relationship between the reflection loss development and microstructural changes in the mortar/concrete, which initiate the compressive strength development.

The S-ΔR_L regression lines of the mortar batches are given in Fig. 7. As it can be expected from the similarity of the appropriate reflection loss curves in Fig. 3, the slopes of the three lines have a very small deviation. The S-ΔR_L relationships for concrete in Fig. 8 show clearly different slopes.

The parameter m of all S-ΔR_L relationships, the percentage standard deviation s of the slopes of the regression lines within the concrete and mortar batches and the coefficient of determination r^2 for each regression are listed in Table 3. The standard deviation of m for the mortar batches is with 3.1 % less than one fourth of that for the concrete batches (13.39 %). Hence, in contrast to concrete, mortar seems to have a material specific S-ΔR_L relationship. However, the r^2 values in Table 3, which represent the fraction of the variance of compressive strength that is explained by the regression lines (Moore 1995) presented in Fig. 7 and 8, show that the accuracy of the strength prediction is not affected by this phenomenon. All r^2 values are calculated for the combination of one single batch and its regression line.

The derived S-ΔR_L relationships can now be used to predict the compressive strength from the measured reflection loss. The measured versus predicted strength values for the mortar and concrete experiments are shown in Fig. 9. The predicted strength values are calculated based on the m-values for each single batch.

The application of the strength prediction procedure as shown requires the estimation of the coefficient m of the S-ΔR_L relationship. If the strength of concrete is determined by direct measurements at the beginning of the strength development, the value of m can be calculated. This value can now be used for the prediction of the further strength gain, since m has been shown to be constant for the relevant period of time. Consequently the prediction procedure presented in this paper requires reliable compressive strength values determined by common compression tests in the first 24 hours of the concrete age. These values can be considered as calibration values, which include the specific properties of the tested concrete composition. The accuracy of the strength prediction is intimately related to the reliability of these calibration values.

ACCURACY OF STRENGTH PREDICTION AND COMPARISON TO OTHER METHODS

The accuracy of the proposed strength prediction is governed by the coefficient of determination r^2 of the S-ΔR_L relationships, which is given in Table 3. To allow a comparison with other methods, the correlation coefficient r_{cor}, the standard error of estimate (SEE) and the relative standard error of estimate (RSEE) of the strength estimates are calculated. The correlation coefficient measures the strength of the relationship between predicted and experimental strength (Moore 1995) and can be calculated either from the S-ΔR_L or S_{pred}-S_{meas} data. The standard error of estimate is the square root of the average of the squared prediction residuals over the prediction period. The relative standard error of estimate is the ratio of SEE and the average of the calculated strength values (Popovics 2001). The r_{cor} value, SEE and RSEE for the mortar and concrete batches as a whole as well as for the entirety of the experiments are given in Table 4.

The statistical parameters indicating the accuracy of the strength prediction for a selection of other nondestructive test methods are presented in Table 5. The comparison of the accuracy of the prediction presented in this paper (Table 4) with the data in Table 5, shows that the wave reflection method lies in the upper level. At this point the authors reemphasize that the shown accuracy of the strength prediction represents the maximum potential of the presented method and could only be achieved by using the beforehand determined strength development for

calibrating the used S-ΔR_L relationships. Differences also exist in the length of the prediction period of the proposed method (3 days) and the methods given in Table 5. Nevertheless, the presented accuracy reveals the excellent capability of the wave reflection method to follow the strength gain of mortar and concrete at early ages.

CONCLUSION

Based on the investigations presented in this paper, the following conclusions can be drawn:

1. Wave reflection measurements on mortar are repeatable concerning shape and final value of the reflection loss curve. Measurements on concrete can reproduce the time of occurrence of distinct points in the reflection loss graph, but not the final value. Consequently, wave reflection measurements depend on local material properties (such as coarse aggregate ratio, water to cement ratio) of the material at the measurement point. Relatively homogeneous materials, such as mortar, give a unique reflection loss development.
2. Compressive strength and reflection loss for the tested mortar and concrete mixtures are linearly related for early ages.
3. Multiple measurements with the same mortar mixture gave almost unique S-ΔR_L relationships, with only a small deviation in their slopes. Repeated experiments with the same concrete gave different S-ΔR_L relationships.
4. Once the S-ΔR_L relationship is determined, it can be used to predict the compressive strength gain of mortar or concrete at constant temperature conditions with a high accuracy ($r>0.99$) based only on the measured reflection loss. Separate S-ΔR_L relationships were used to predict the strength development for each single batch of the mortar and concrete mix.
5. The inflection point (point of maximum slope) in the reflection loss curve is related to the initiation of the compressive strength development. This indicates that the wave reflection method can measure microstructural changes in cementitious materials, which are crucial for the development of compressive strength. Further research has to be conducted to specify these relationships.
6. The strength prediction presented herein is based on S-ΔR_L relationships calculated from a number of strength values determined by compression tests. For practical application of the method it will be necessary to determine of the S-ΔR_L relationships from the measured reflection loss and common strength tests performed in the first 24 hours after casting. At the present state of the research the relationship among the time of occurrence of the inflection point (t_i) in the reflection loss graph and the time of strength initiation (t_s) can not be used for the strength prediction because of its instability.
7.

ACKNOWLEGDEMENT

The presented research was funded by the Center for Advanced Cement-Based Materials and the Infrastructure Technology Institute of Northwestern University. The support of these institutions is gratefully acknowledged by the authors.

APPENDIX I. REFERENCES

Akkaya, Y., Voigt, Th., Subramaniam, K.V., Shah, S.P. (2002), "Nondestructive measurement of concrete strength gain by an ultrasonic wave reflection method." *Materials and Structures,* in press.

Bickley, J.A. (1982). "The variability of pullout tests and in-place concrete strength." *Concrete International,* 4(4), 44-51.

Chotard, T., Gimet-Breart, N., Smith, A., Fargeot, D., Bonnet, J.P., Gault, C. (2001). "Application of ultrasonic testing to describe the hydration of calcium aluminate cement at the early age." *Cement and Concrete Research,* 30(3), 405-412.

Di Maio, A.A., Traversa, L.P., Giovambattista, A. (1985). "Nondestructive combined methods applied to structural concrete members." *Cement, Concrete, and Aggregates,* 7(2), 89-94.

Kopf, R.J., Cooper, C.G. (1981). "In situ strength evaluation of concrete case histories and laboratory investigations." *Concrete International,* 3(3), 66-71.

Krautkrämer, J., Krautkrämer, H. (1990). "Ultrasonic testing of materials." Springer Verlag, Berlin, New York, 17.

Moore, D.S. (1995). "The basic practice of statistics." W.H Freeman and Company, New York, 137.

Nasser, K.W., Al-Manaseer, A.A. (1987). "Comparison of nondestructive testers of hardened concrete." *ACI Materials Journal*, 84(5), 374-380.

Öztürk, T., Rapoport, J., Popovics, J.S., Shah, S.P. (1999). "Monitoring the setting and hardening of cement-based materials with ultrasound." *Concrete Science and Engineering,* 1(2), 83-91.

Papadakis, E.P. (1968). "Buffer-rod system for ultrasonic attenuation measurements." *Journal of Acoustical Society of America,* 44(5), 1437-1441.

Pessiki, P., Johnson, M.R. (1996). "Nondestructive evaluation of early-age concrete-strength in plate structures by the impact-echo method." *ACI Materials Journal,* 93(3), 260-271.

Popovics, S. (2001). "Analysis of the concrete strength versus ultrasonic pulse velocity relationship." *Materials Evaluation,* 59(2), 123-129.

Quasrawi, H.Y. (2000). "Concrete strength by combined nondestructive methods simply and reliably predicted." *Cement and Concrete Research,* 30(5), 739-746.

Rapoport, J., Popovics, J.S., Subramaniam, K.V., Shah, S.P. (2000). "The use of ultrasound to monitor the stiffening process of portland cement concrete with admixtures." *ACI Materials Journal,* 97(6), 675-683.

Samarin, A., Meynik, P. (1981). "Use of combined ultrasonic and rebound hammer method for determining strength of concrete structural members." *Concrete International,* 3(3), 25-29.

Stepišnik, J., Lukač, M., Kocuvan, I. (1981). "Measurement of cement hydration by ultrasonics." *Ceramic Bulletin,* 60(4), 481-483.

Valič, M.I. (2000). "Hydration of cementitious materials by pulse echo USWR method, apparatus and application examples." *Cement and Concrete Research,* 30(10), 1633-1640.

Valič, M.I., Stepišnik, J. (1998). "A study of hydration of cement pastes by reflection of ultrasonic shear waves. Part I: Apparatus, experimental method and application examples." *Kovine, Zlitine, Tehnologije,* 32(6), 551-560.

Valič, M.I., Stepišnik, J. (1999). "Applications of pulsed USWR method for materials studies." *Kovine, Zlitine, Tehnologije,* 33(5), 341-344.

APPENDIX II. NOTATION

The following symbols are used in this paper:

d_1, d_2 = material and geometric losses of transducer signal;

d_3, d_4 = material and geometric losses of first reflection;

$F_1(f)$, $F_2(f)$ = fast Fourier transform of first and second reflection;

$F_{1,free}(f)$, $F_{2,free}(f)$ = fast Fourier transform of first and second reflection for the free boundary case;

FFT = fast Fourier transform;

G = shear modulus;

m = slope of the S-ΔA relationship;

r = reflection coefficient at steel concrete/mortar interface;

$\bar{r}$ = reflection coefficient at transducer-steel interface;

R_1, R_2 = first and second reflection from steel-concrete/mortar interface;

R_L = reflection loss;

$R_{L,crit}$ = critical reflection loss value for calculation of change in reflection loss;

r^2 = coefficient of determination;

r_{cor} = correlation coefficient;

RSEE = relative standard error of estimate;

s = standard deviation;

S = compressive strength;

S_{meas} = measured compressive strength

S_{pred} = predicted compressive strength

SEE = standard error of estimate;

S_T = transducer signal;

T_1, T_2 = first and second transmission through steel-concrete/mortar interface;

t_i = time of occurrence of the inflection point;

t_s = time when strength starts to increase;

v = wave velocity;

ΔA = change of reflection loss;

ρ = mass density;

Figure Captions

FIG. 1. Schematic Representation of the Multiple Reflection and Transmission Process at the Steel-Concrete Interface

FIG. 2. Time (a) and Frequency Domain (b) of the Acquired Wave Reflections with F_1, F_2 as the FFT of the First and Second Reflection

FIG. 3. Reflection Loss Development of the Three Mortar Batches

FIG. 4. Reflection Loss Development of the Three Concrete Batches

FIG. 6. Determination of the S-ΔR_L Relationship

FIG. 7. S-ΔR_L Relationships for Mortar Batches

FIG. 8. S-ΔR_L Relationships for Concrete Batches

FIG. 9. Measured vs. Predicted Strength for (a) Mortar and (b) Concrete

Table Captions

TABLE 1. Mixture Proportions by Weight of Cement of the Tested Mortar and Concrete

TABLE 2. Time Values t_d, t_s and their Ratios

TABLE 3. Parameters of S-ΔR_L Relationships

TABLE 4: Standard Error and Relative Standard Error of Estimate of the Calculated Predictions

TABLE 5. Accuracy of Strength Prediction of Several Nondestructive Test Methods

TABLE 1. Mixture Proportions by Weight of Cement of the Tested Mortar and Concrete

Mix (1)	Cement (2)	Water (3)	Gravel (4)	Sand (5)	Fly ash (6)
Mortar	1	0.50	0	2.42	0.26
Concrete	1	0.52	2.62	2.42	0.26

Note: Superplasticizer both mixes: 0.93 %weight of cement

TABLE 2. Time Values t_i, t_s and their Ratios

Batch (1)	t_i (hours) (2)	t_s (hours) (3)	t_s/t_i (4)
(a) Mortar			
M-1	12.51	9.40	0.75
M-2	13.13	9.60	0.73
M-3	12.88	9.49	0.74
(b) Concrete			
C-1	16.12	10.70	0.66
C-2	16.72	12.20	0.73
C-3	16.67	11.30	0.68

TABLE 3. Parameters of S-ΔR_L Relationships

Batch (1)	m (2)	s of m (%) (3)	r^2 (4)
(a) Mortar			
M-1	19.064	3.10%	0.988
M-2	19.454		0.991
M-3	18.065		0.995
(b) Concrete			
C-1	14.652	13.39%	0.981
C-2	20.414		0.987
C-3	18.369		0.996

TABLE 4: Standard Error and Relative Standard Error of Estimate of the Calculated Predictions

Prediction (1)	r_{cor} (3)	SEE (MPa) (4)	RSEE (%) (5)
Mortar (M-1,2,3)	0.9957	1.15	3.82
Concrete (C-1,2,3)	0.9945	1.52	5.17
all	0.9950	1.35	4.54

TABLE 5. Accuracy of Strength Prediction of Several Nondestructive Test Methods

Method (1)	Correlation coefficient r_{cor} (2)	Prediction period (days) (3)	Investigator (4)
Pulse Velocity	0.840	28	Nasser and Al-Manasser (1987)[a]
	0.978	- -	Quasrawi (2000)[a]
	0.921	90	Di Maio et al. (1985)[a]
	0.870	- -	Samarin and Meynik (1981)[a]
	0.866	14	Kopf and Cooper (1981)[a]
	0.998	28	Pessiki and Johnson (1996)[b]
Rebound Hammer	0.920	28	Nasser and Al-Manasser (1987)
	0.938	- -	Quasrawi (2000)
	0.919	90	Di Maio et al. (1985)
	0.920	- -	Samarin and Meynik (1981)
	0.929	14	Kopf and Cooper (1981)
Pulse Velocity + Rebound Hammer	0.950	- -	Samarin and Meynik (1981)[a]
	0.975	- -	Quasrawi (2000)[a]
	0.965	90	Di Maio et al. (1985)
Pull-out	0.940	28	Nasser and Al-Manasser (1987)
	0.940	7	Bickley (1982)
	0.982	14	Kopf and Cooper (1981)
Probe Penetration	0.910	28	Nasser and Al-Manasser (1987)
	0.988	14	Kopf and Cooper (1981)

[a] Pulse velocity determined by through transmission method
[b] Pulse velocity determined by impact-echo method

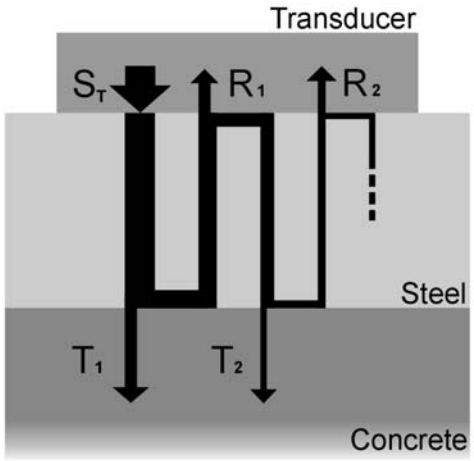

FIG. 1. Schematic Representation of the Multiple Reflection and Transmission Process at the Steel-Concrete Interface.

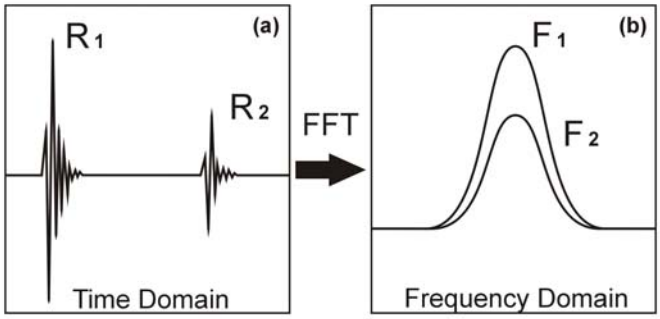

FIG. 2. Time (a) and Frequency Domain (b) of the Acquired Wave Reflections, F_1, F_2 – FFT of First and Second Reflection

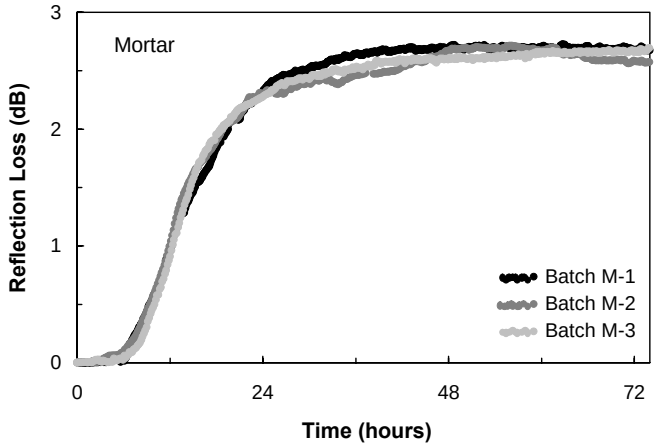

FIG. 3. Reflection Loss Development of the three Mortar Batches

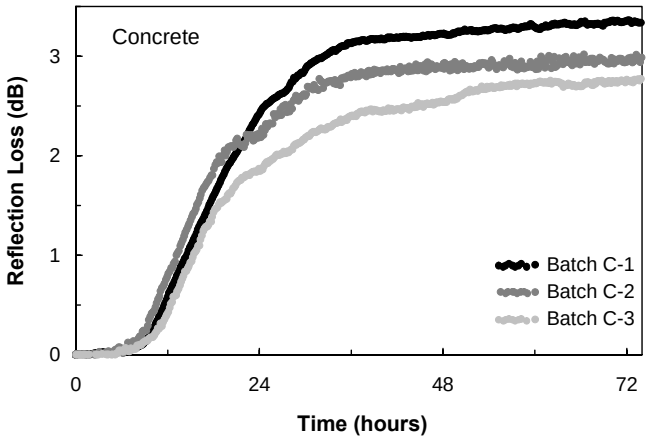

FIG. 4. Reflection Loss Development of the three Concrete Batches

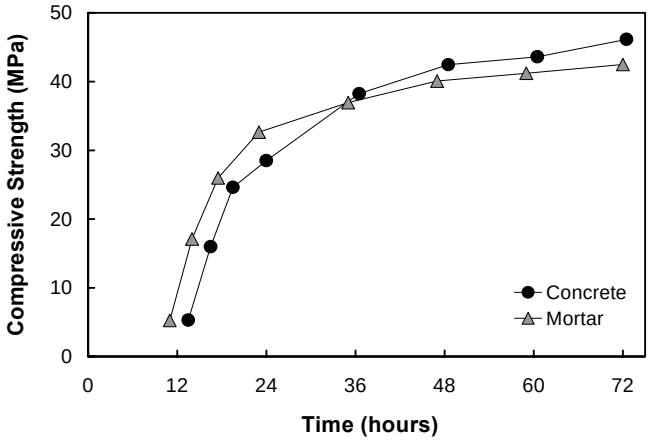

FIG. 5. Compressive Strength Development of Mortar and Concrete Mixtures

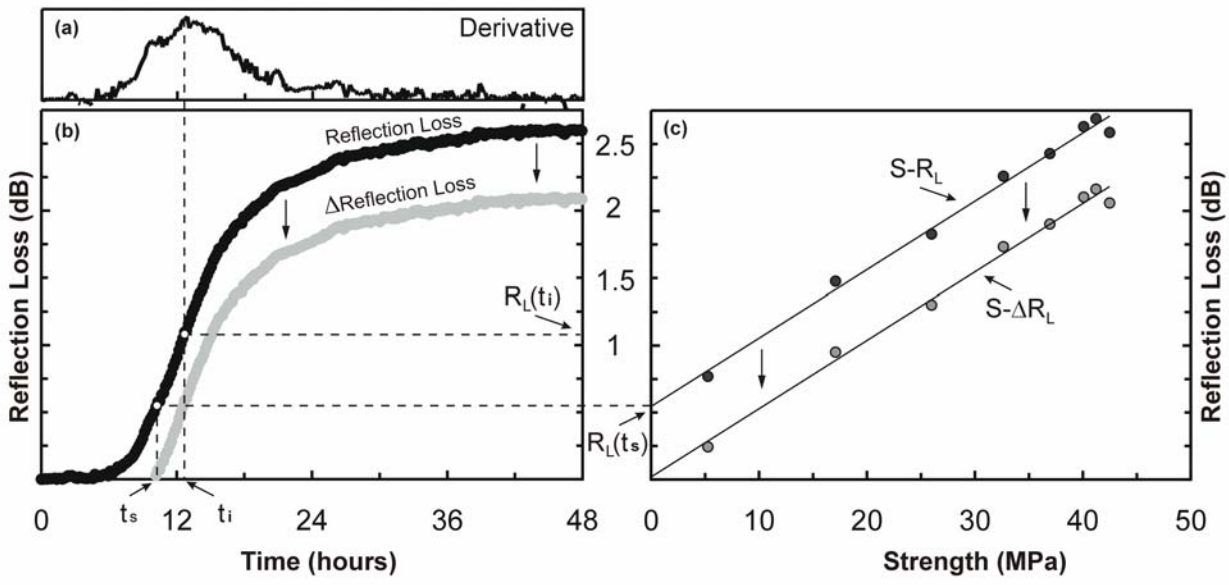

FIG. 6. Determination of the S-ΔR_L Relationship for Mortar Batch M-2

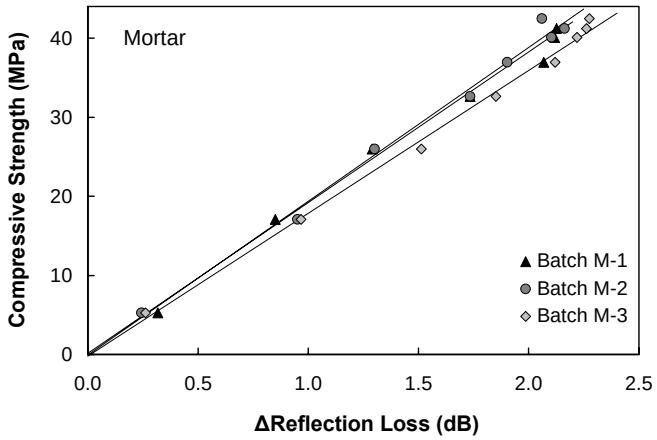

FIG. 7. S-ΔR_L Relationships for Mortar Batches

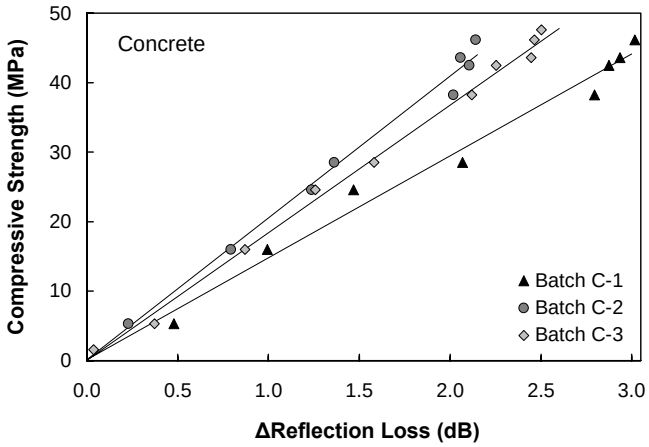

FIG. 8. S-ΔR_L Relationships for Concrete Batches

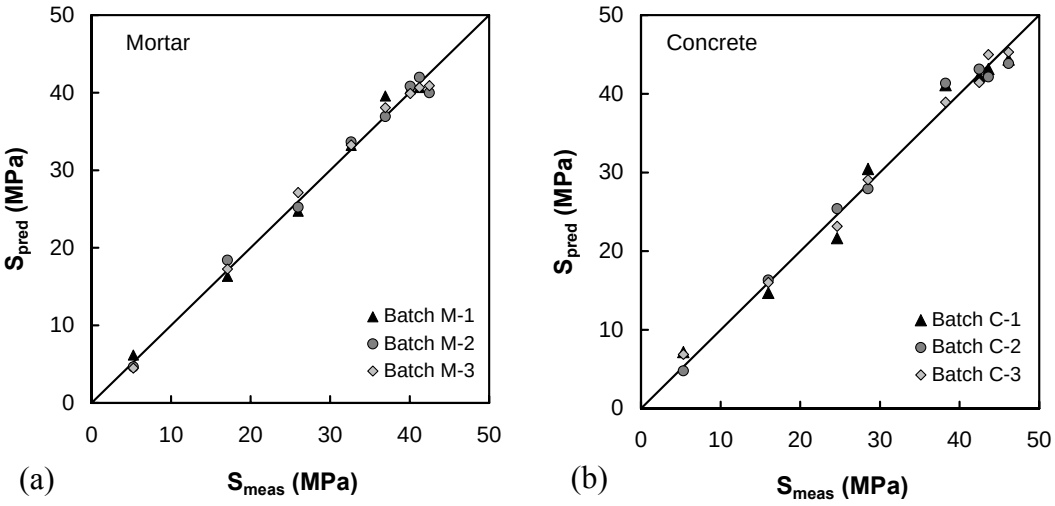

FIG. 9. Measured vs. Predicted Strength for (a) Mortar and (b) Concrete